Spitzer Bubble と星形成

2018/07/05 河野 樹人

Spitzer bubble

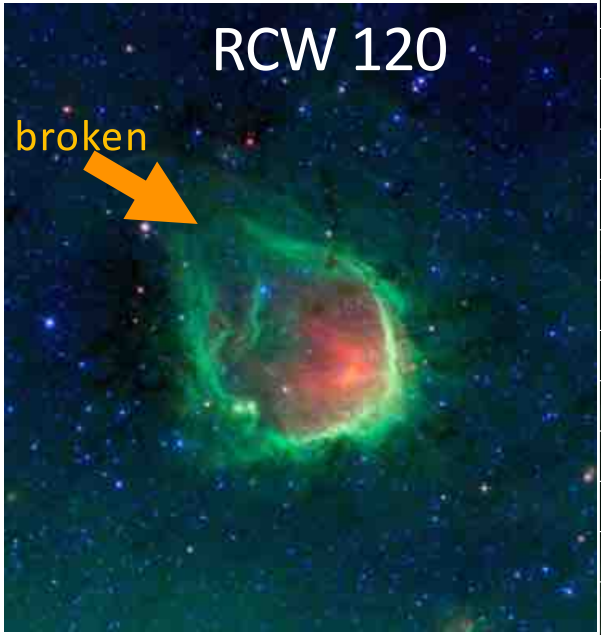

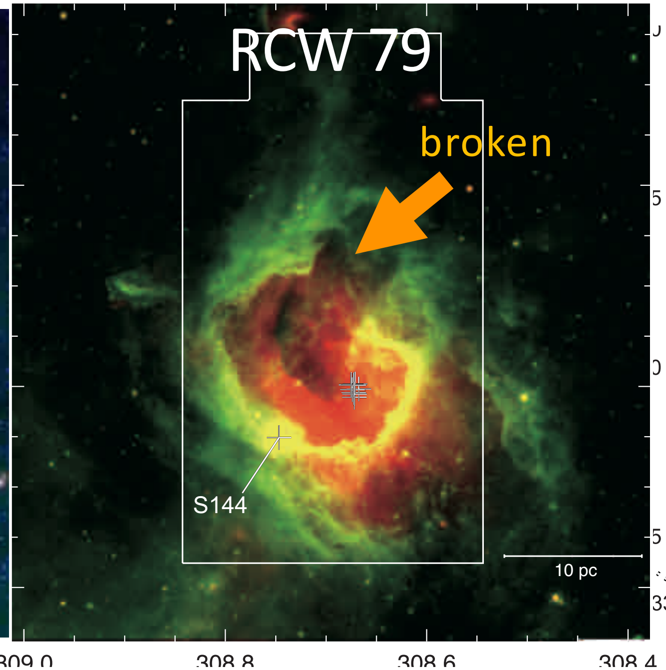

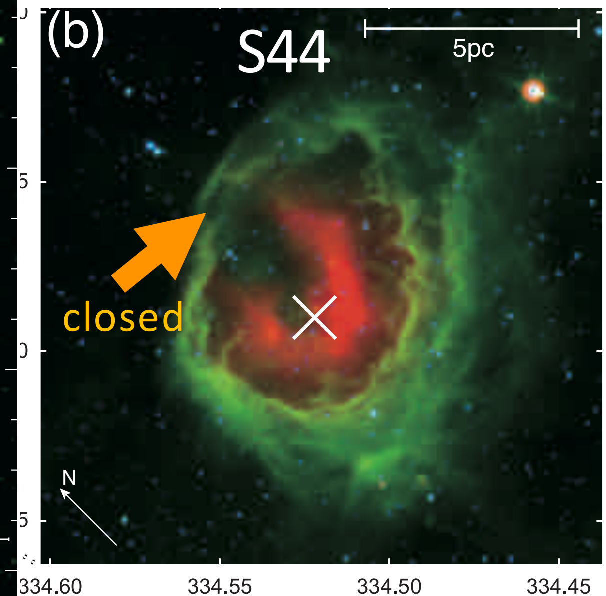

- GLIMPSEデータを用いてChurchwell+06,07 によって同定
- 大部分は大質量星を内包したHII領域
- 8 um (PAH + hot dust)でシェル構造
- 主な種類(赤外線データからのmorphology による分類)
  - Closed, Broken, Bipolar, Multipleなど

Spitzer bubble

Bipolar bubble

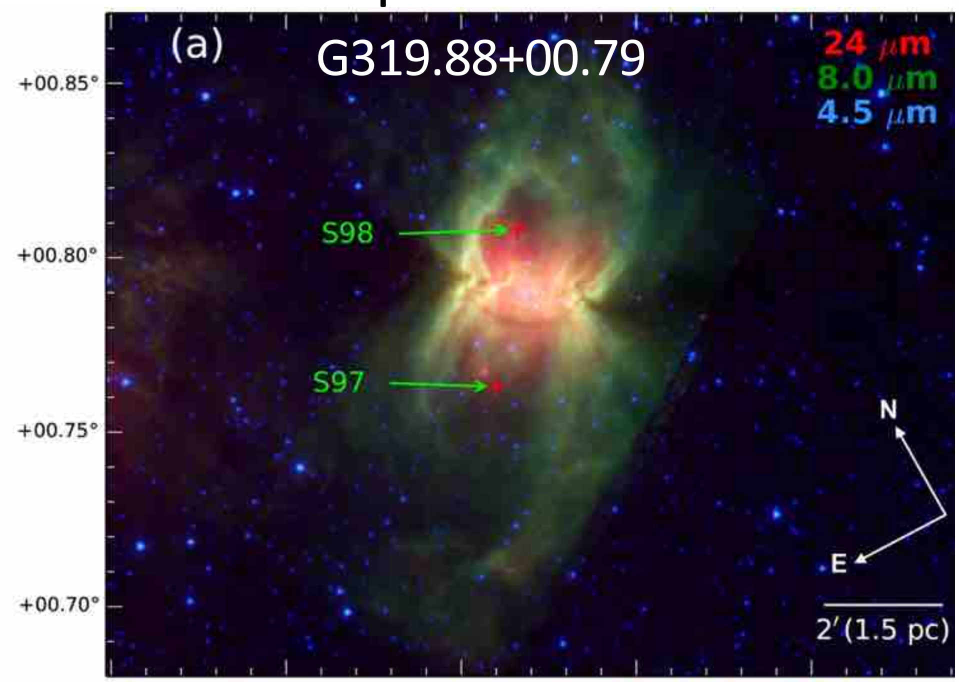

Multiple bubble

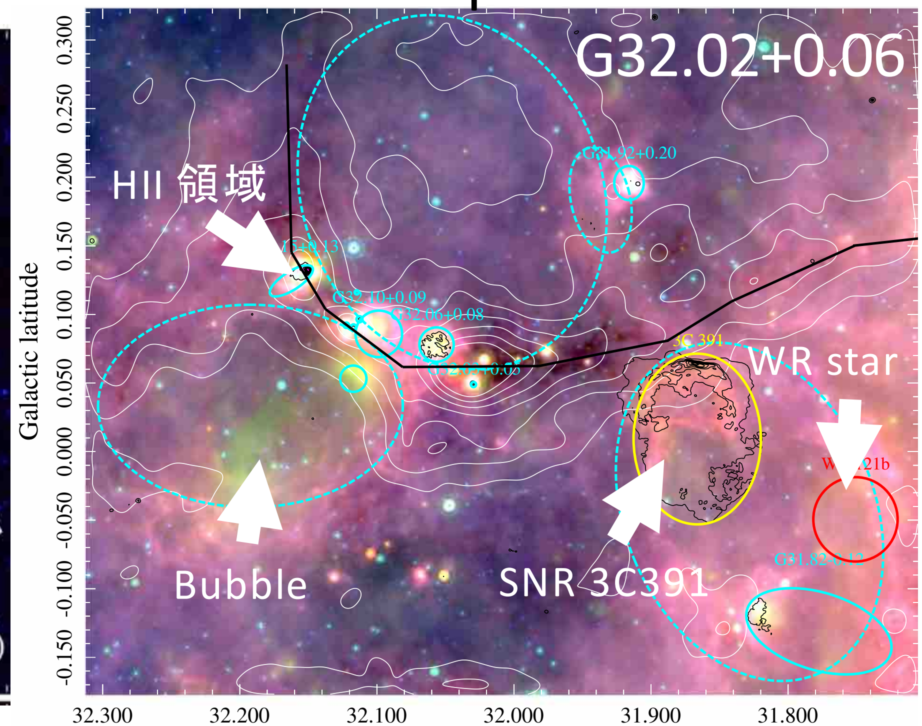

Blue:8 um, Green : 24um, red 70 um: Battersby+2014

- GLIMPSEデータを用いてChurchwell+06,07 によって同定
- 大部分は大質量星を内包したHII領域
- 8 um (PAH + hot dust)でシェル構造
- 主な種類(赤外線データからのmorphology による分類)
  - Closed, Broken, Bipolar, Multipleなど

THE INFRARED MILKY WAY: GLIMPSE/MIPSGAL (3.6–24 microns)

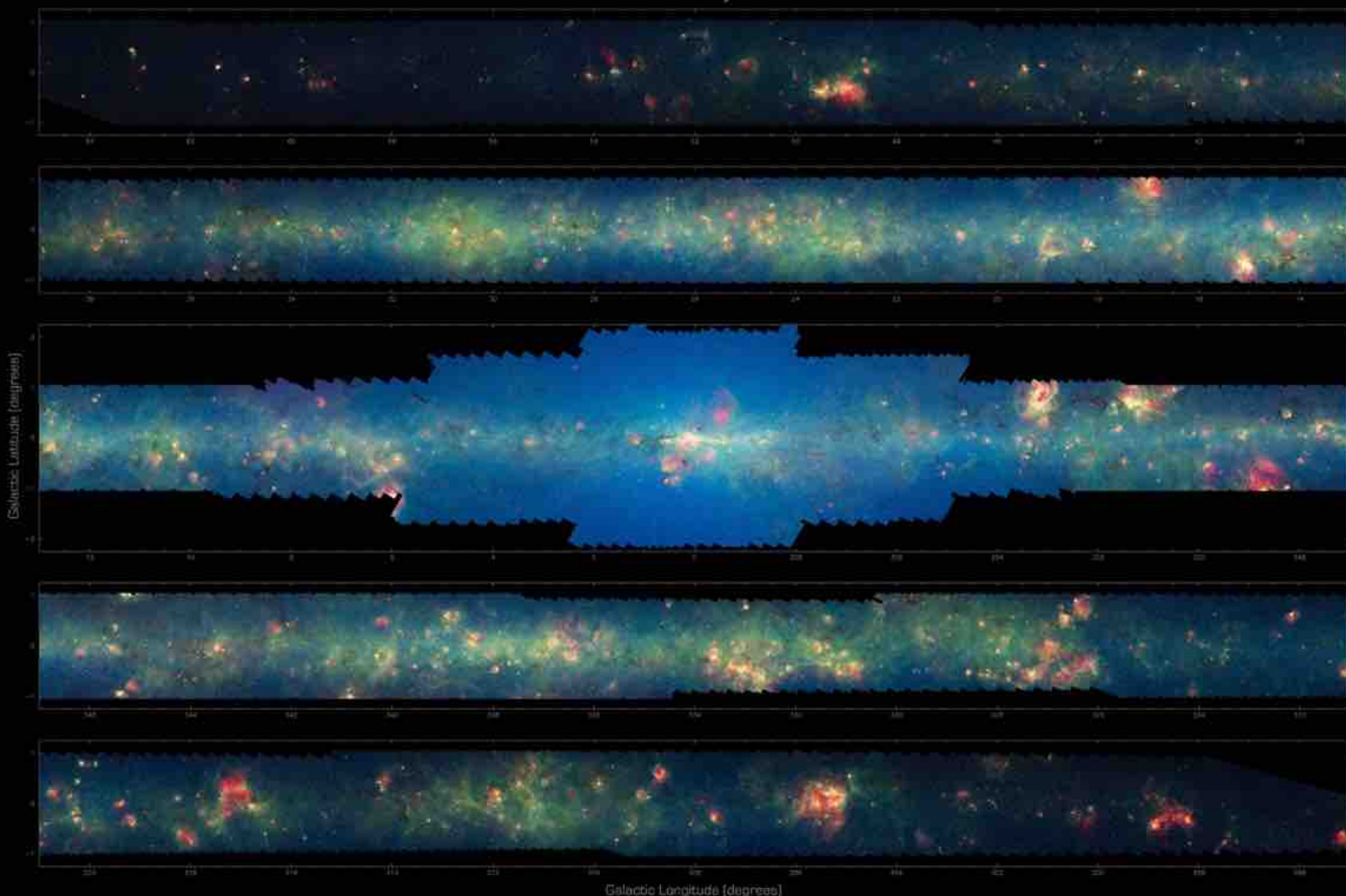

Spitzer bubble と星形成シナリオ

1.HII領域の膨張による誘発的星形成

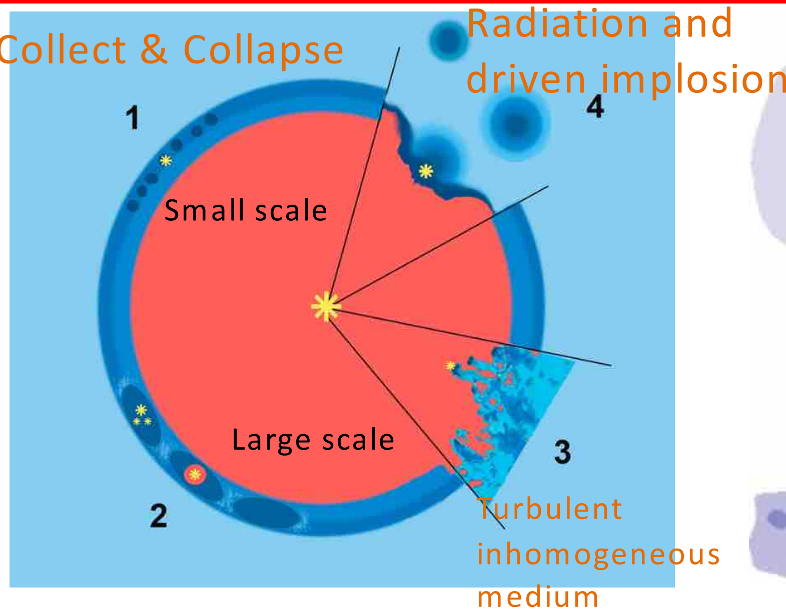

Deharveng+10

2. シート状分子雲による
リング構造

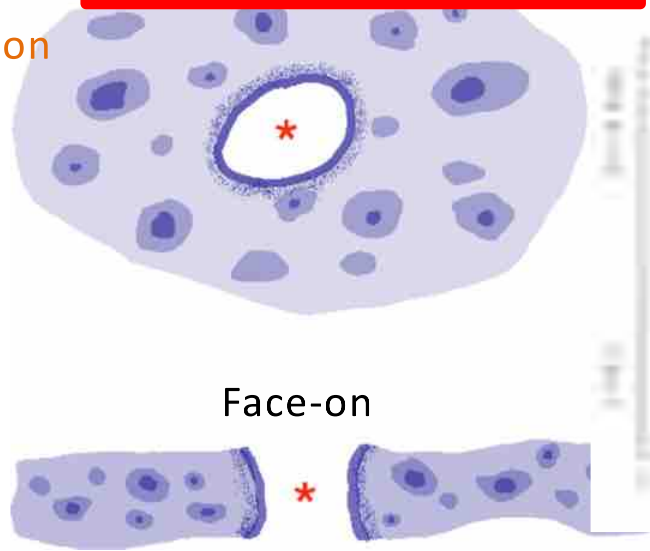

Beaumont & Williams 2010

3. 分子雲衝突による
バブル形成

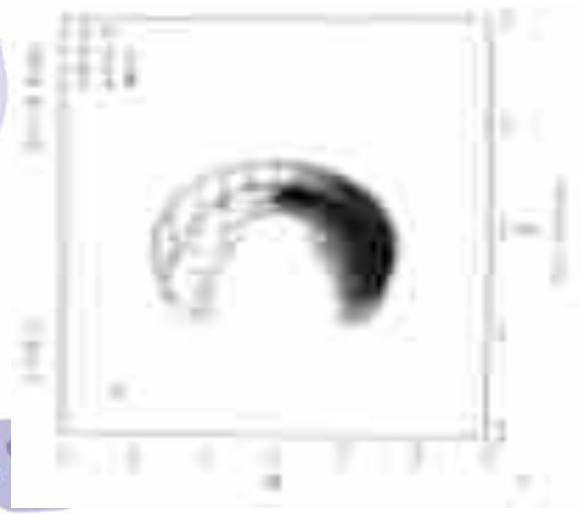

Habe & Ohta 1992

1. 膨張シェルによる周囲の星間物質の掃き集めが星形成を誘発
2. COの速度構造から膨張運動が観測されない-> リング構造??
3. 分子雲同士の衝突によってバブルが形成

これらは本当に対立する仮説なのか?
全てのバブルが同じメカニズムで形成されているのか?

バブルの中心と端での星形成

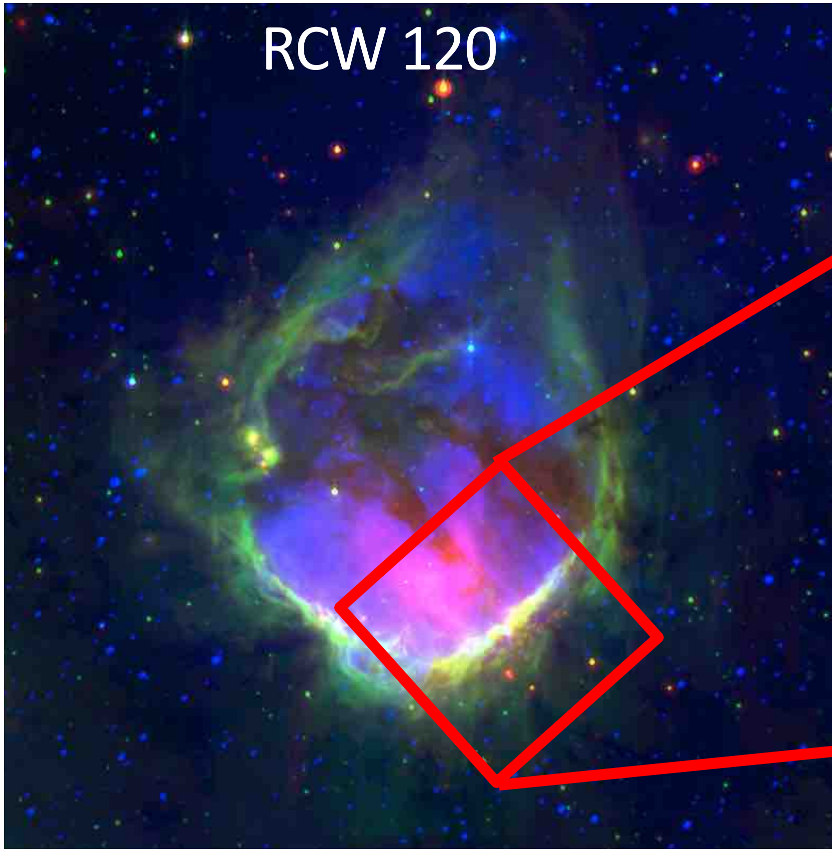

Blue : Hα, green : 8 um, red : 24 um

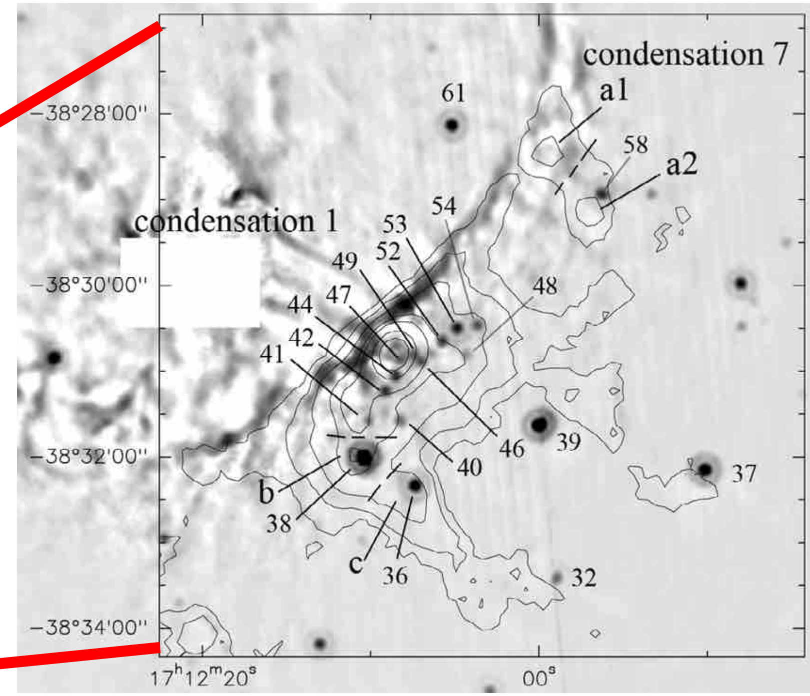

Image : 24 um
Contour : 870 um

Deharveng+10

- バブルの端で、cold dust condensation が形成
- YSO の集中

バブル中心の励起星形成と端での次世代の星形成メカニズムは同じ?

孤立したバブルとMultipleなバブル

S44

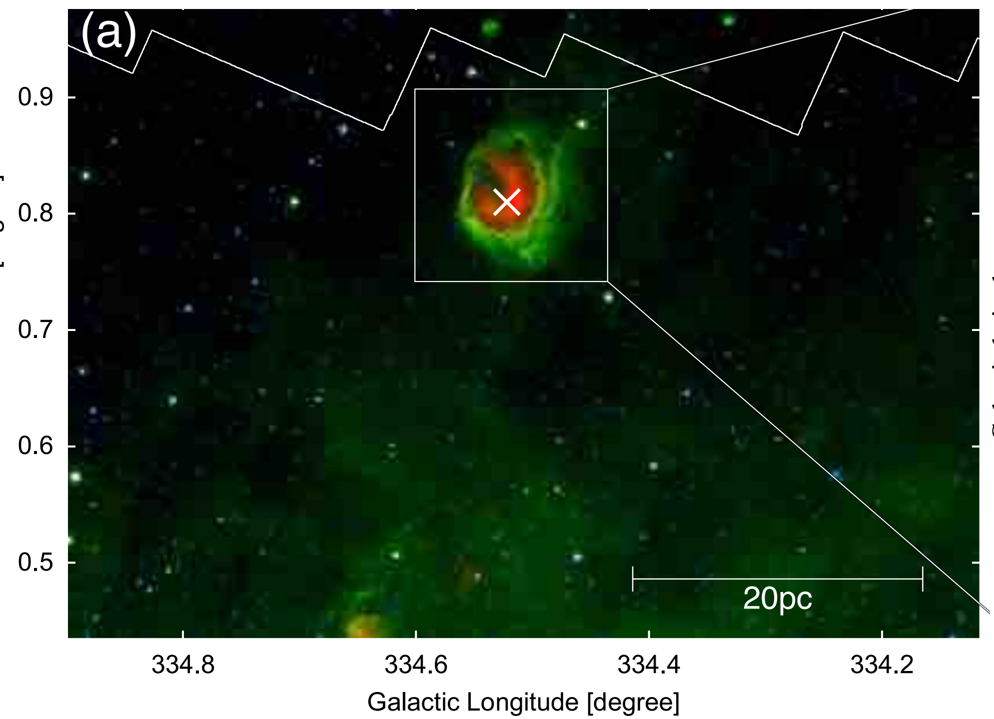

Blue : 3.6 um, Green:8 um, red 24 um

G32.02+0.06

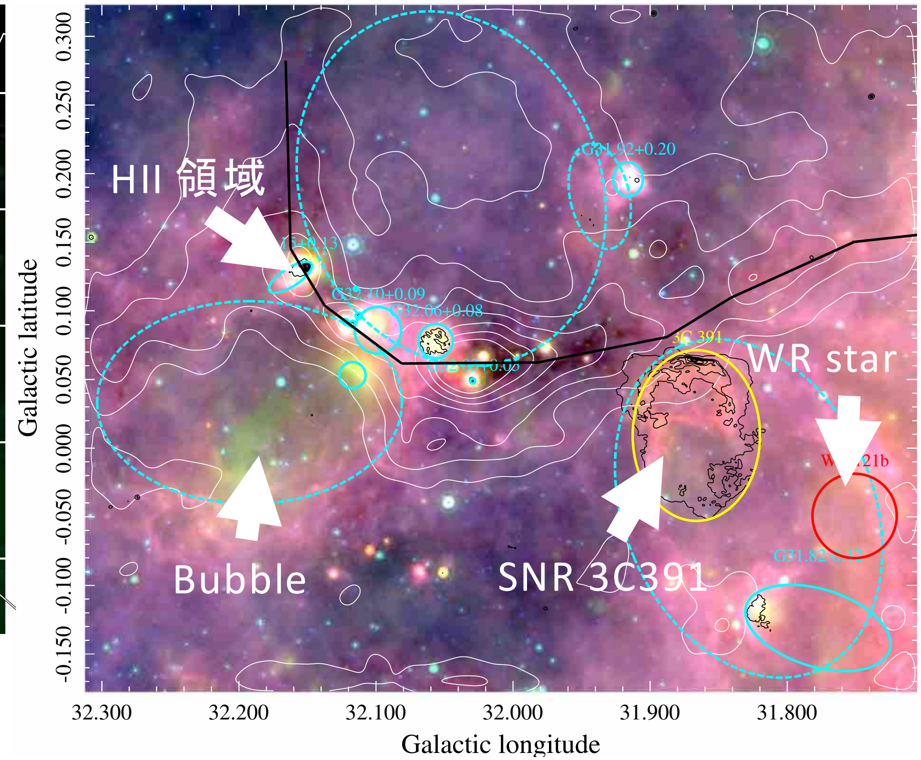

Blue:8 um, Green : 24um, red 70 um: Battersby+2014

- 周囲 20 pcにわたって他の星形成領域がない孤立したバブルS44
- SNRを含む複数のバブルで形成された星形成領域 G32.02+0.06

これらは同じメカニズムで形成されたのか？

観測提案: bipolar バブル G319.88+00.79

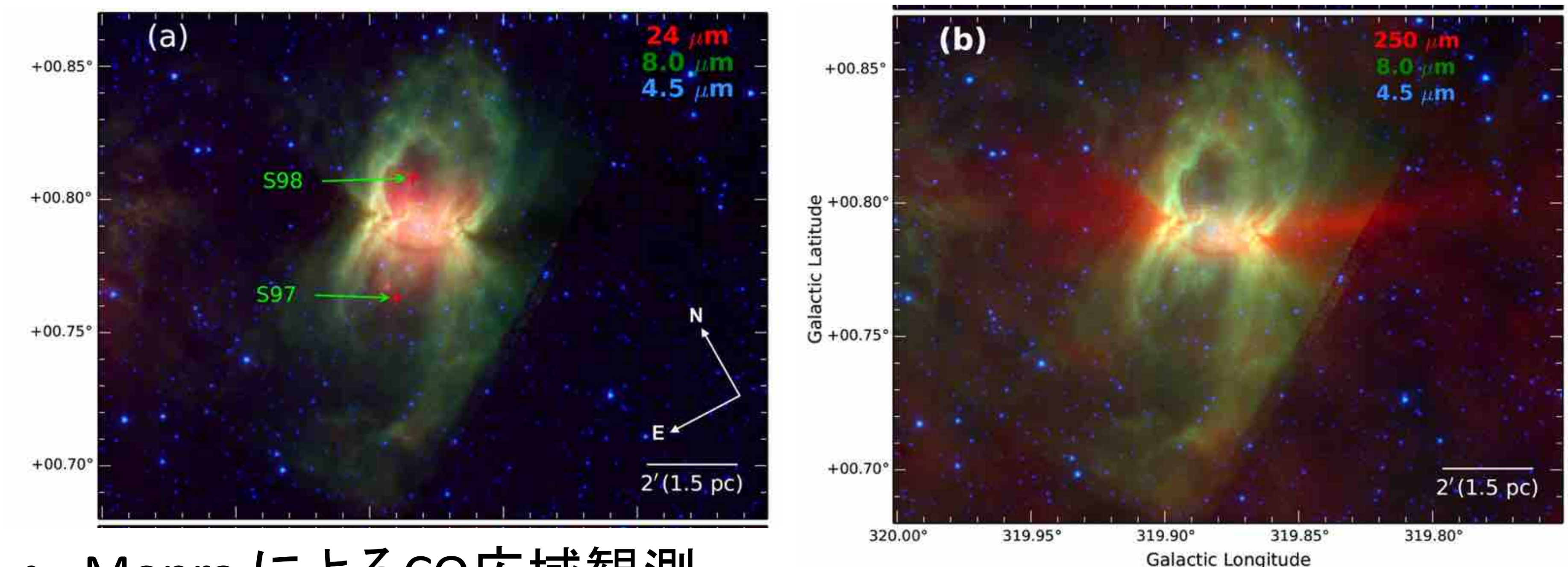

Deharveng+15

- Mopra によるCO広域観測
  - 距離 2.6 kpc
  - NANTEN2ではすでにカバー済み？
  - ASTE では服部さんがすでに観測済み? (要確認)
  - 12CO,13CO,C18O (1-0)
  - 輝線強度比による励起状態の診断
  - 速度方向の解析(膨張運動、ブリッジ成分の有無)
  - RCW 36 (Sano+18) との比較
  - 数値シミュレーションとの比較(Whitworth+)

Deharveng+15の観測結果

- 8umはbipolar に分布
- Cold dustはbipolarに垂直
- 3つのdust condensation
  ->柱密度のpeakに対応
- ダスト温度の分布は8umと概ね一致

速度構造は？

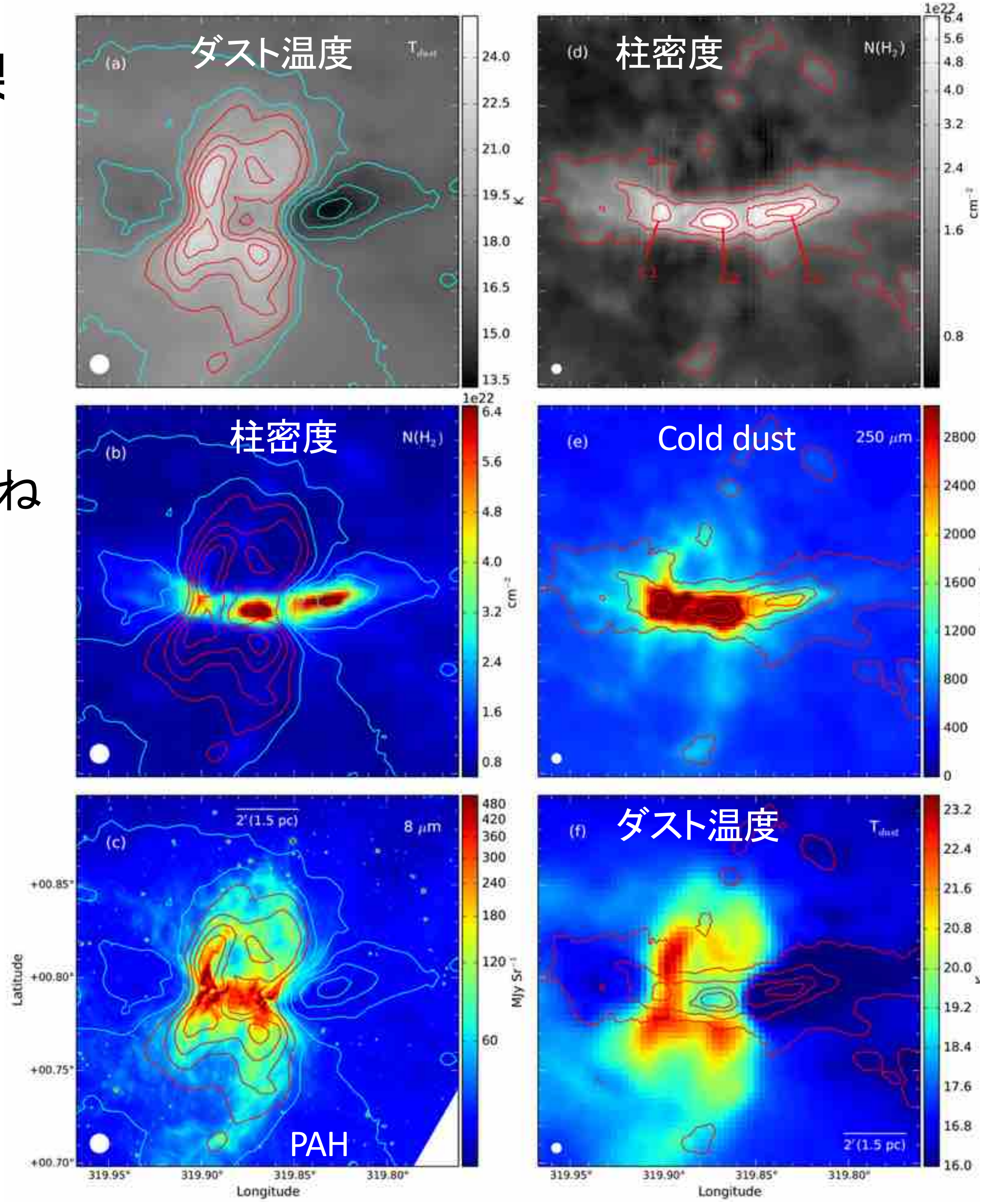

HCO+(1-0) 速度場マップ

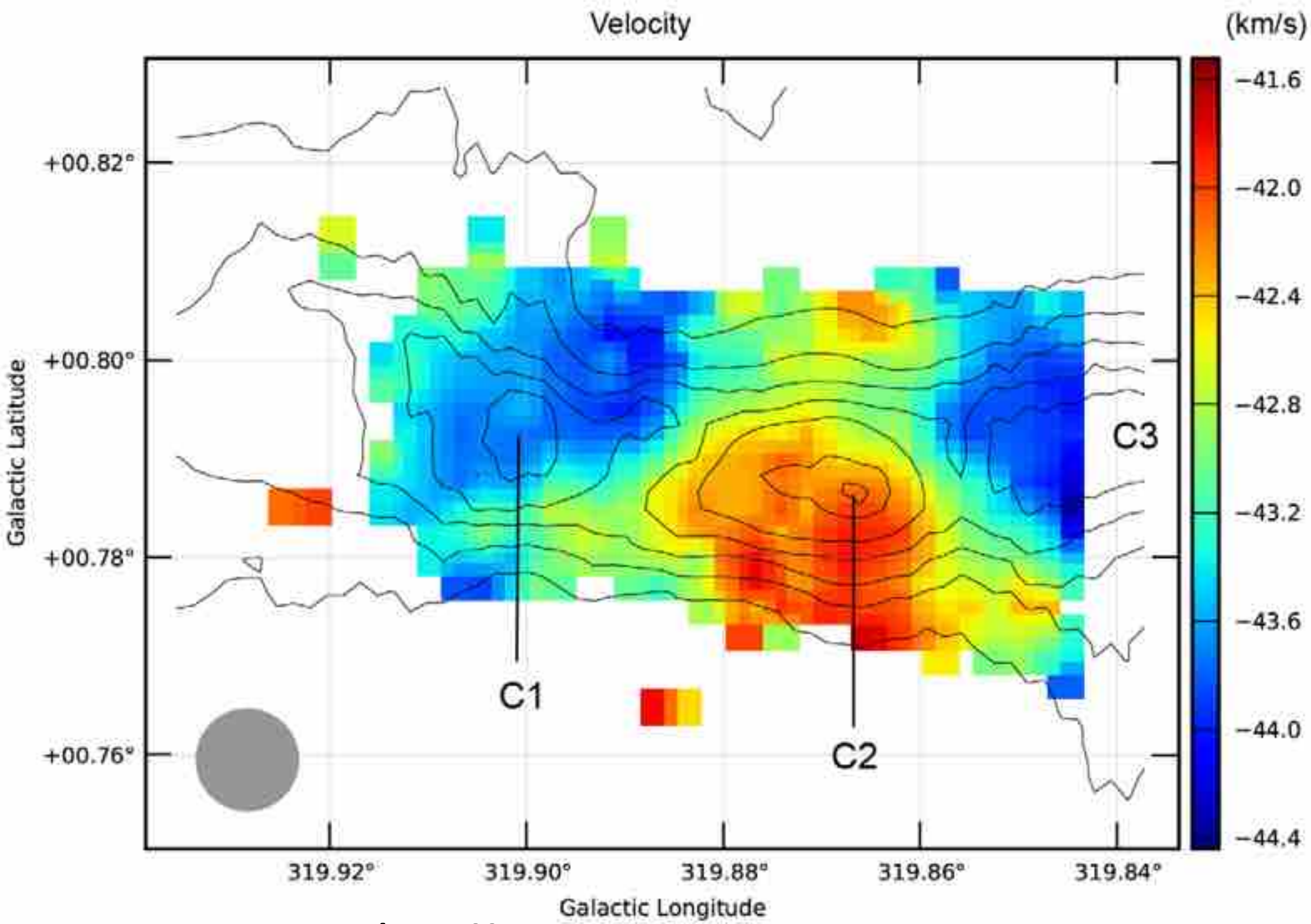

Contour : 柱密度

- Mopra 90 GHz(Millimeter Astronomy Legacy Team)による観測
- クランプ C2とC1,C3の間で速度差 3 km/s

COでbipolar nebula 全体の速度構造を見てみたい

G319.88+00.79 の形成シナリオとmorphology

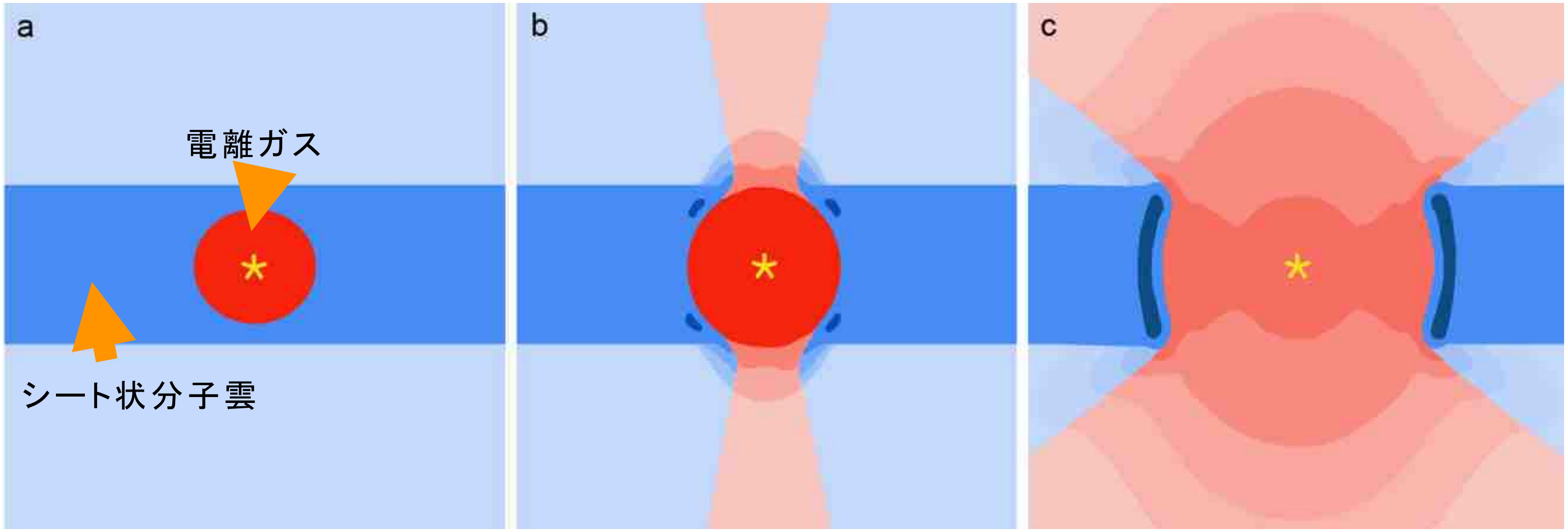

Fig. 1. Formation of a bipolar H II region, according to the simulation of Bodenheimer et al. (1979; their Fig. 4; the thickness of the parental plane is 1.3 pc, its density 300 H_2 cm^{-3}). The ionized material appears in red, the neutral material in blue; the density of the material is indicated by the saturation level. Schema **a)** shows the dense molecular plane surrounded by low density material, the initial Strömgren sphere around its central exciting star ($T_* = 4 \times 10^4$ K). In schema **b)**, at 3×10^4 yrs, the expanding H II region reaches the border of the parental cloud, and the low density material is quickly ionized; a bipolar nebula forms. In schema **c)**, at 1×10^5 yrs, the high density ionized material flows away from the central region; high density molecular material accumulates at the waist of the bipolar nebula, forming a torus of compressed material.

Deharveng+15

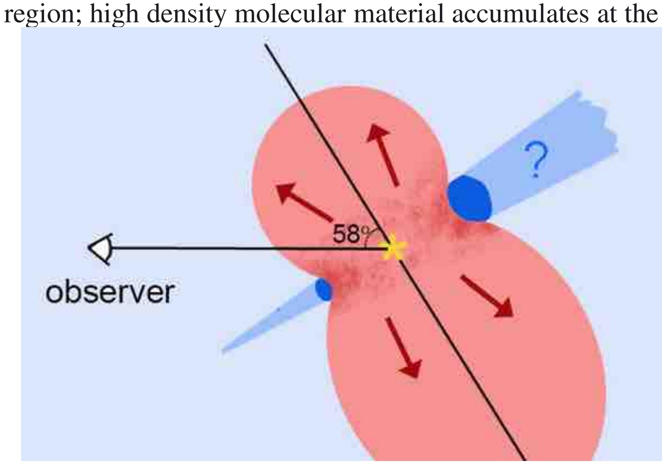

Fig. 27. Morphology of G319.88+00.79. The ionized material appears in pink, the neutral one in blue. We do not know the extent of the molecular material at the back of the nebula.

- 平面状の分子雲で大質量星が形成
- HII領域が球対称に膨張
- シートに対して垂直方向に電離ガスが放出し、bipolar nebulaが形成。シート方向にはトーラス状にガスが圧縮され次世代の星が形成

Bipolar bubbleと分子雲衝突

Bipolar H II regions produced by cloud–cloud collisions

Anthony Whitworth,[1,*] Oliver Lomax,[1] Scott Balfour,[1] Pierre Mège,[2] Annie Zavagno,[2] and Lise Deharveng[2]

One or more of the ionising stars remains close to the midplane of the collision.

Looking close to along the collision axis, the HII region appears cylindrical.

Looking close to across the collision axis, the HII region appears bipolar

Column-density of neutral gas

Emission measure of ionised gas

along

across

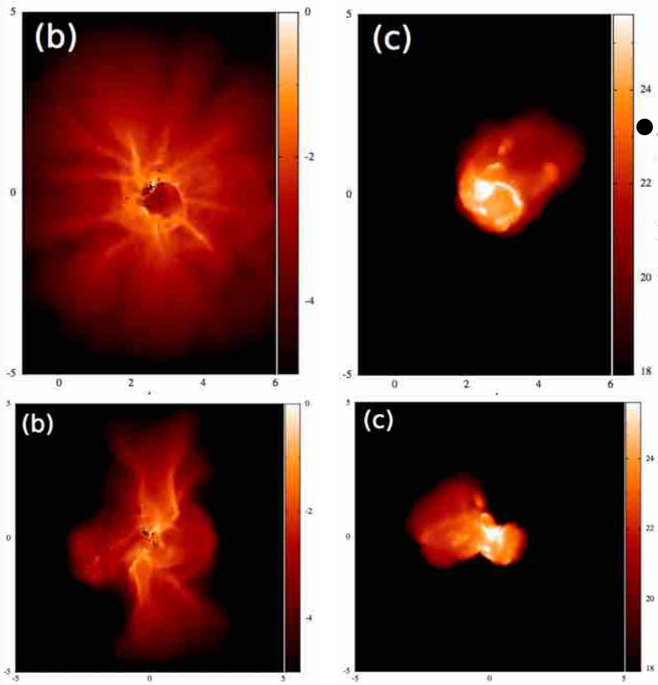

- Bipolar bubbleも分子雲衝突によって解釈可能？
- なぜbipolar に見えるのか？ (初期条件の違い? projectionの違い?)

Ant Whitworth, Cardiff University

VIALACTEA 2016, September 30, Rome

Whitworthスライドより

Star formation by collect and collapse

Apex-LABOCA 870 μm contours unsharp-mask image Spitzer 24 μm

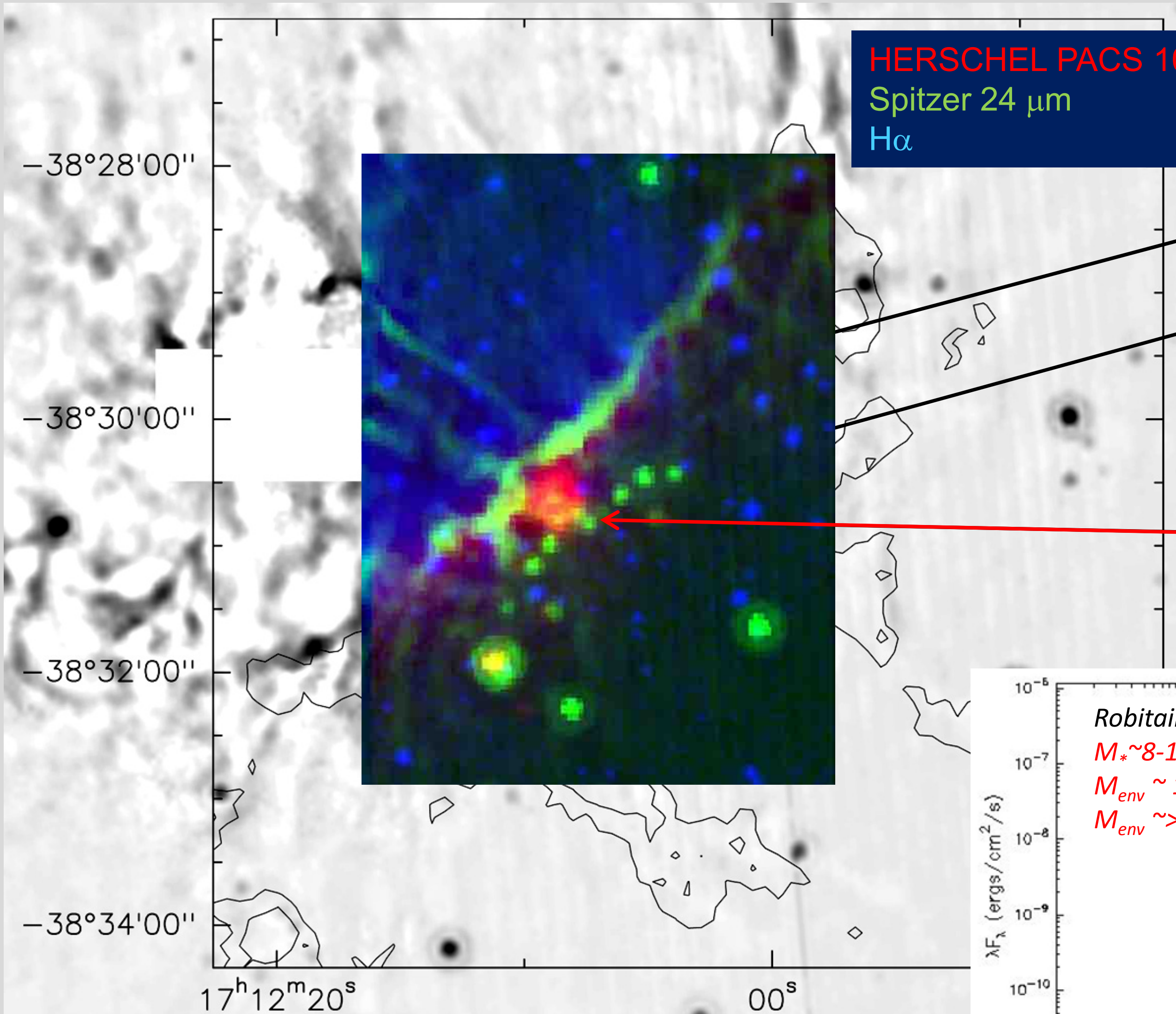

Ionization front

Chain of ~10 YSOs
// to the IF
Class I or I/II

Dense core
detected at 100 μm
Class 0
Zavagno et al. 2010

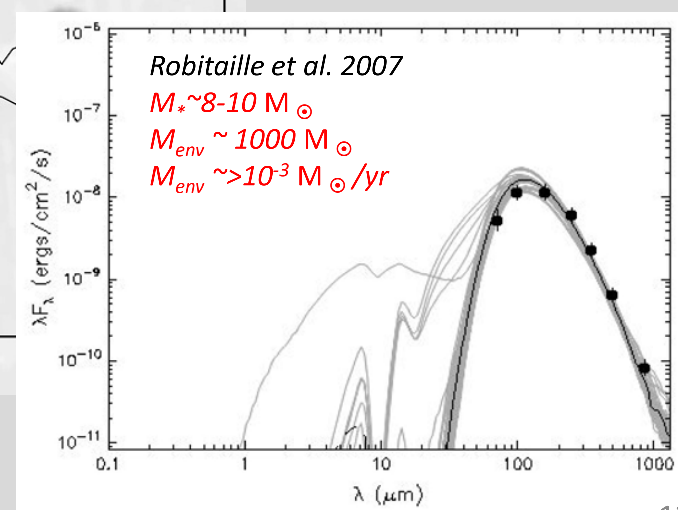

3 - What is the prevalence of massive-star formation triggered by HII regions?

⇒ The ATLASGAL survey shows the cold dust emission at 870 μm, and thus the distribution of the neutral material associated with HII regions *Schuller et al. 2009, A&A, 504, 415*

65 bubbles have enough resolution to study the cold dust distribution

13 bubbles have associated compact or UC HII regions (adjacent to the IF, in the PDR)

6 more have 6.7 GHz associated methanol masers (signature of massive SF)

Thus more than 29% of the HII regions enclosed in bubbles have triggered the formation of massive stars

Deharveng et al., submitted to A&A

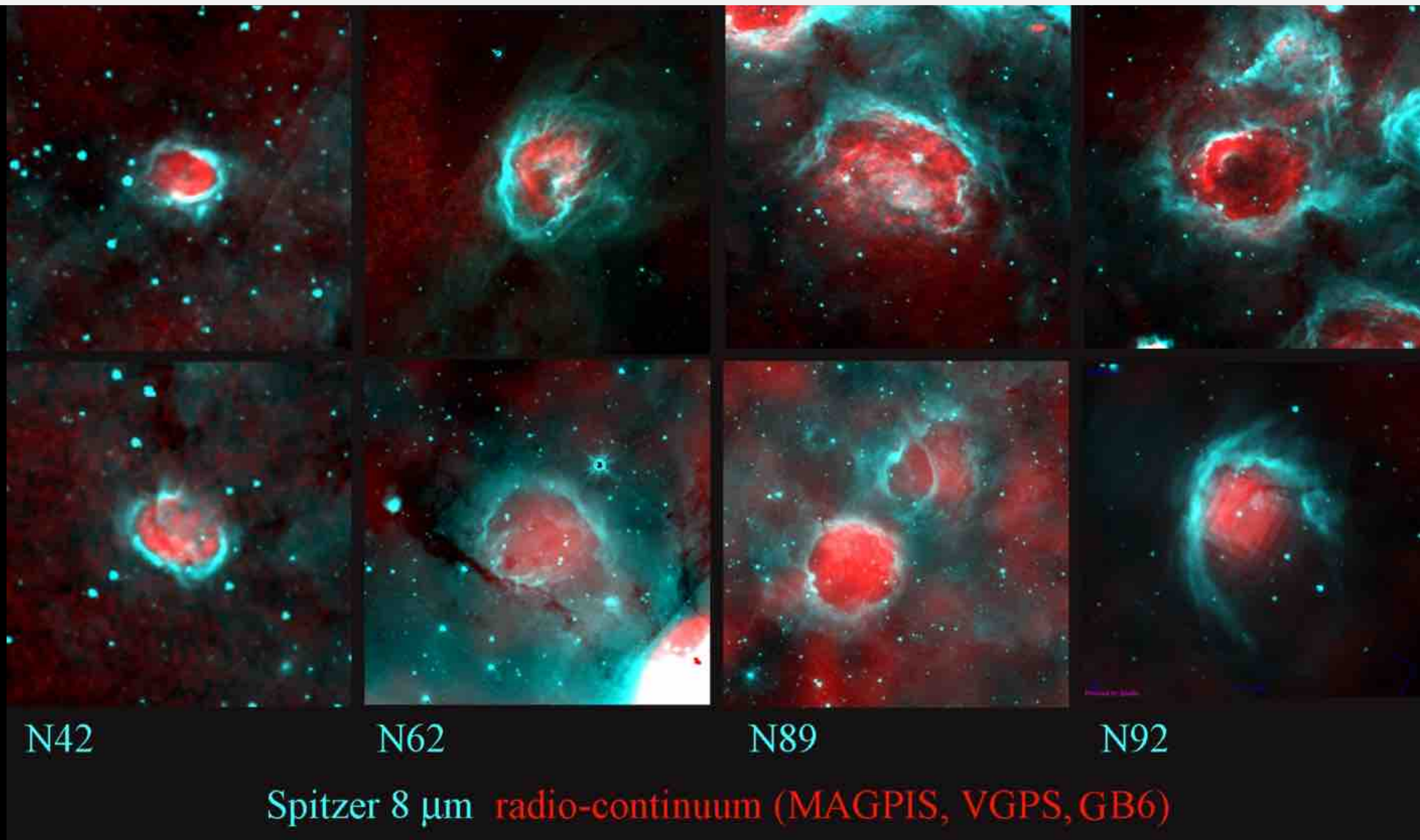

RCW 120の compact source

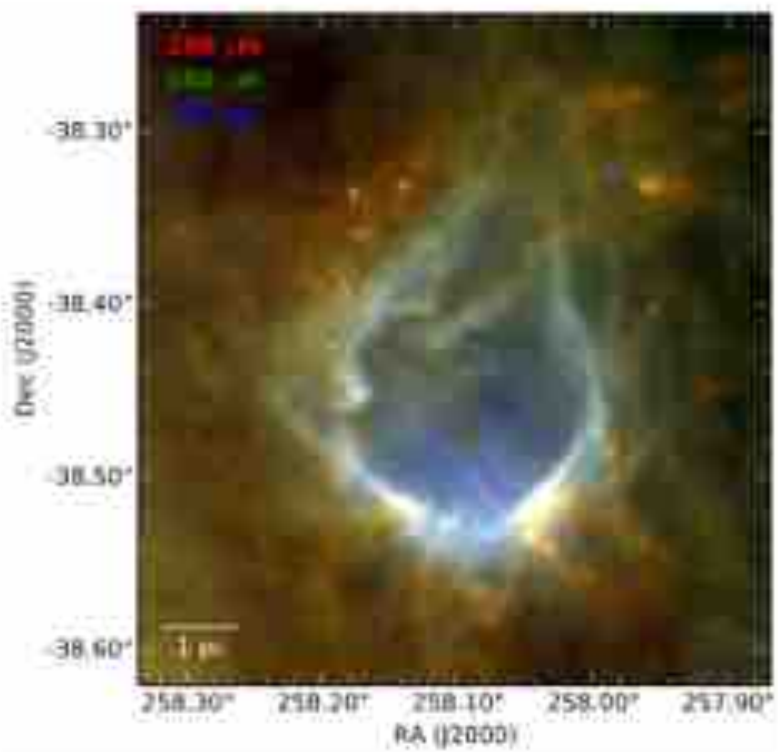

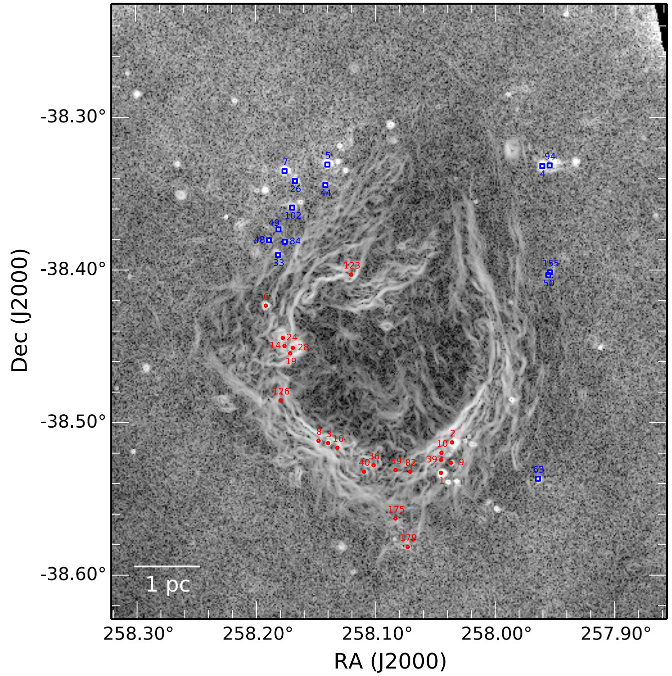

Fig. 6. All 35 compact sources detected using *getsources* (and discussed in the text) superimposed on a 70 μm gradient image of RCW 120. The sources are color-coded depending on their location: red circles for sources observed towards the PDR, blue squares for sources outside (see text).

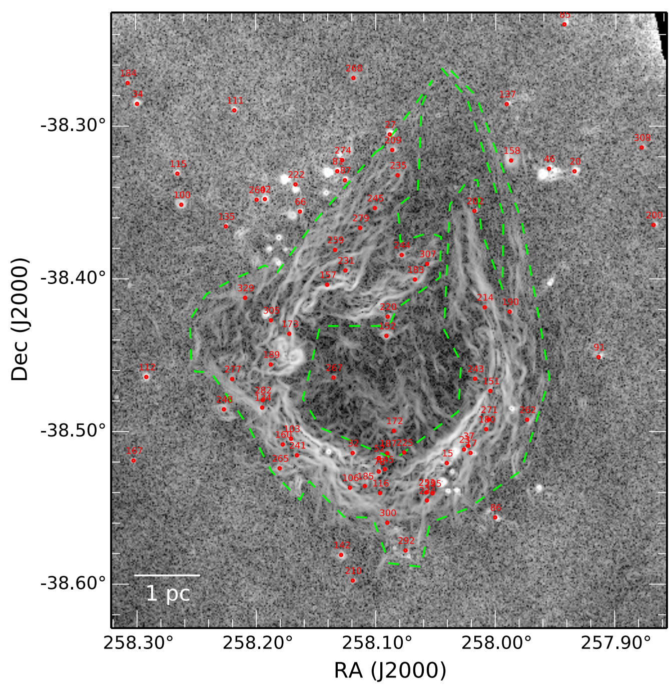

Fig. 7. All 87 sources detected by *getsources* but not part of the final sample due to the lack of reliable flux measurements, mainly at SPIRE wavelengths. Physical parameters of these sources are derived in a secondhand way explained and presented in Sect. 5.2.4. The PDR region is enclosed in the green countours (see text).

Figueira+2017

RCW 79 のcompact source

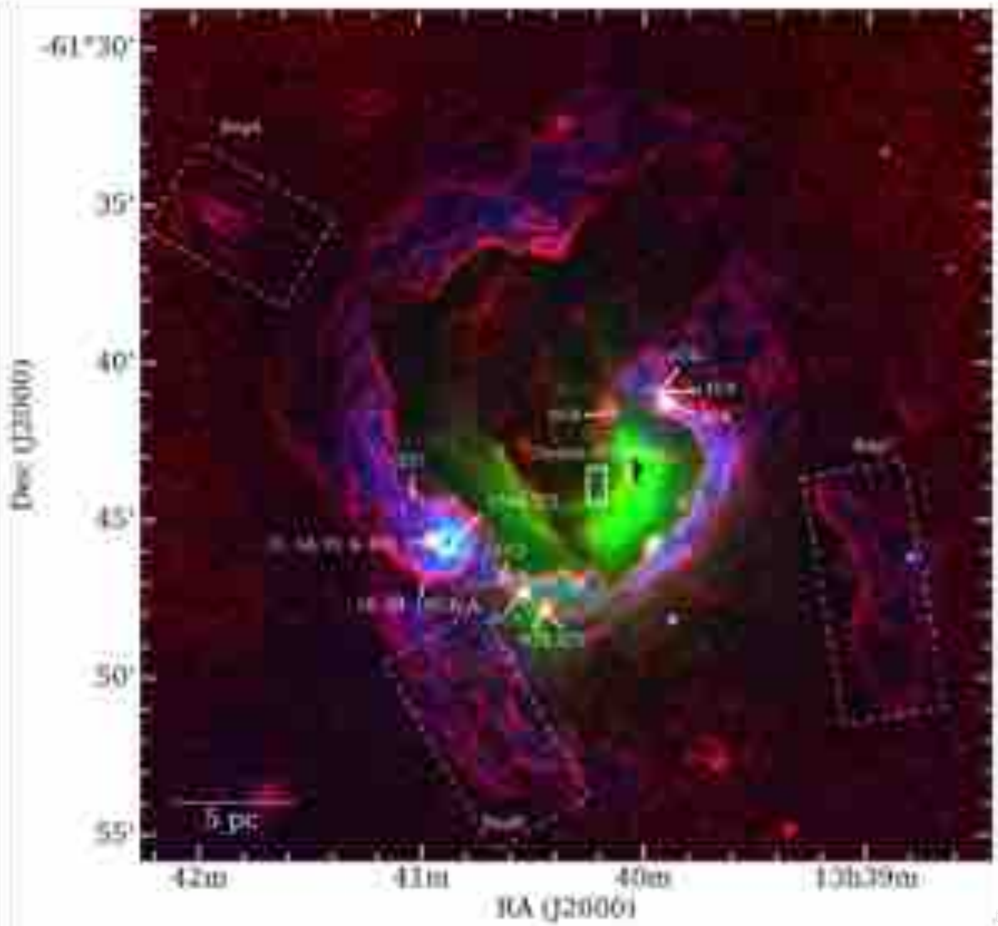

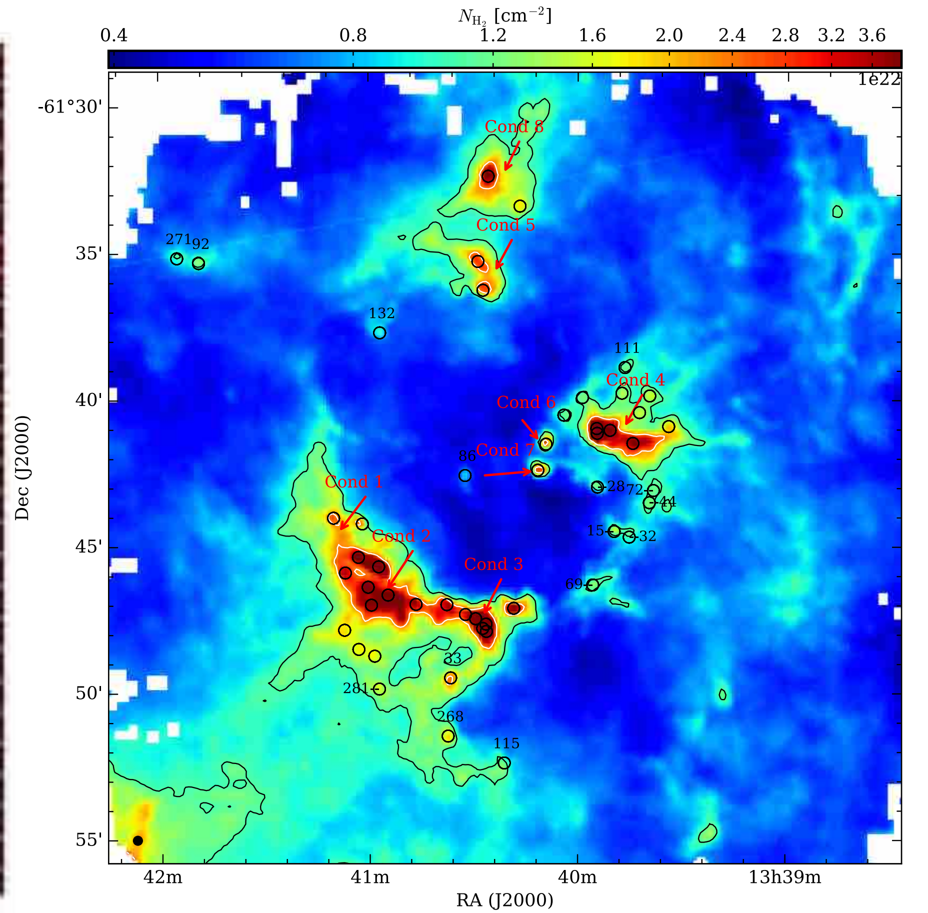

ribution of 50 compact sources overlaid on the high-resolution (18.″2) column density map. The bl
white contours delineate the gas in the compressed layer (above $N_{H_2} = 11 \times 10^{21}$ cm^{-2} marked with the black
and the gravitationally dominated gas (above $N_{H_2} = 23 \times 10^{21}$ cm^{-2} marked with the white contour, see S
respectively. The arrows pinpoint the eight condensations as named by ZA06. A beam size of 18.″2 is shown
black full circle on the bottom left.

Liu+2017

RCW 79 のcompact source

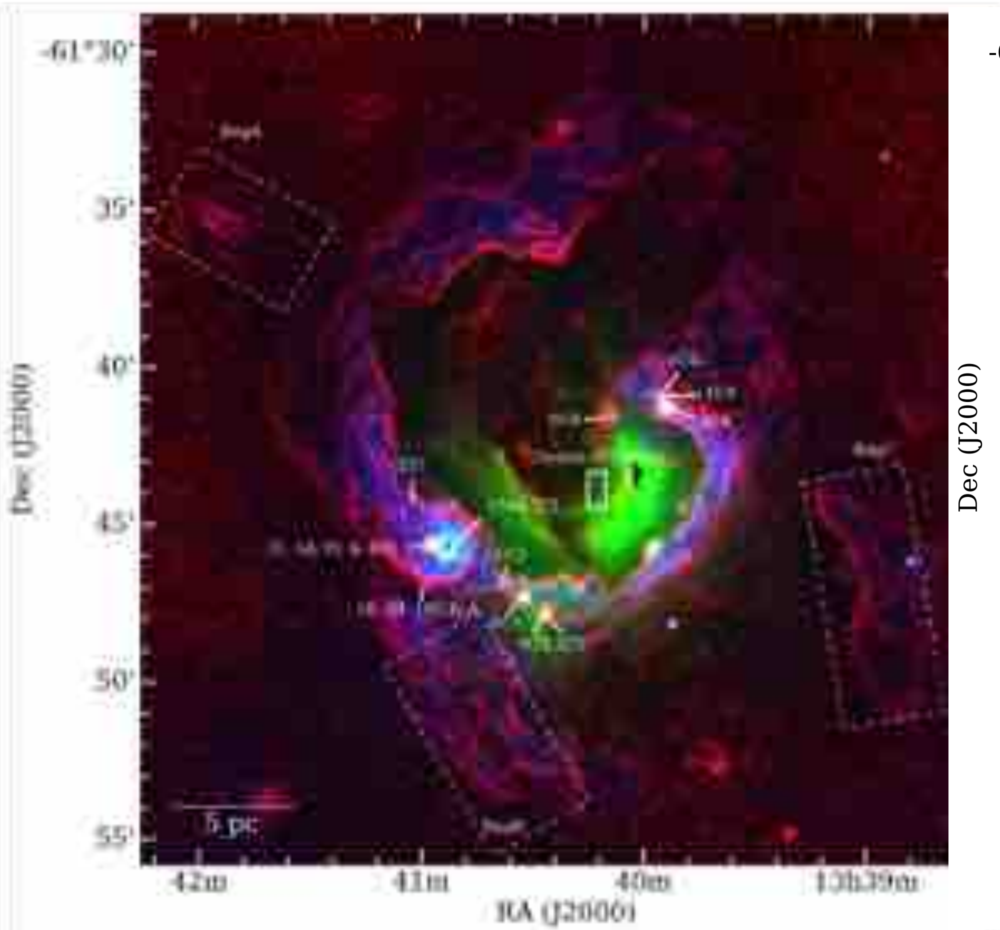

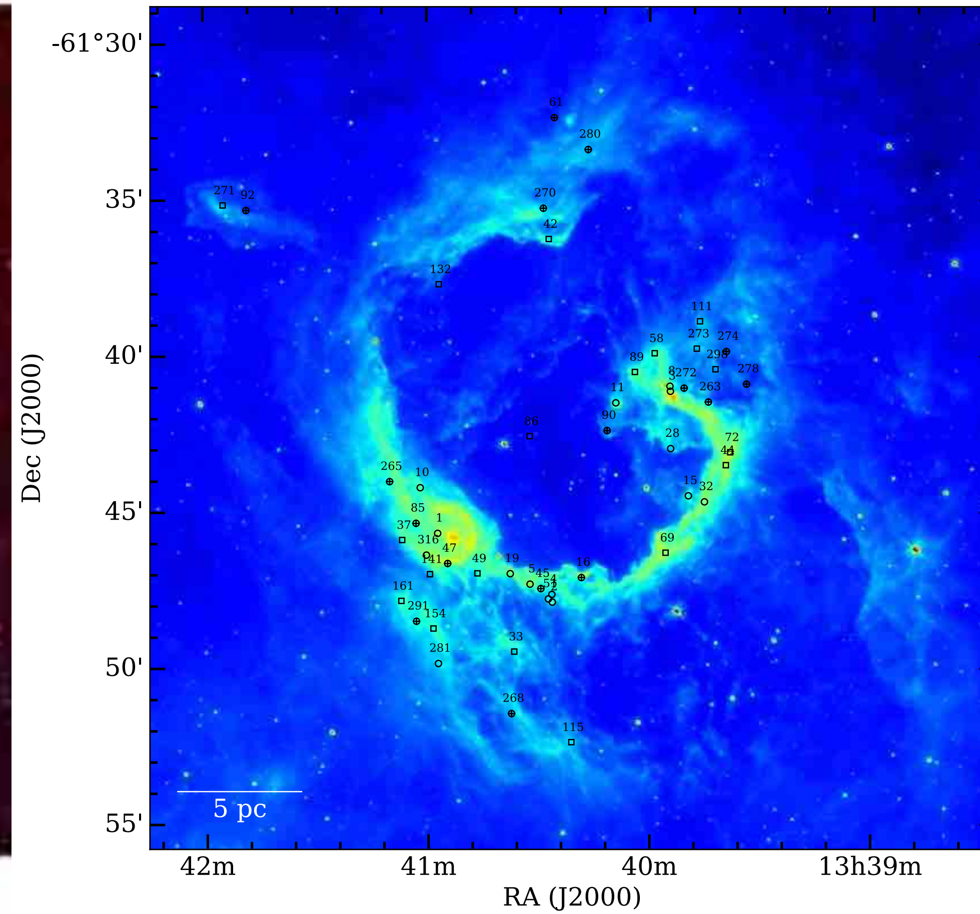

Blue : 8um, green : 24 um, red 70 um

Fig. 12: Fifty compact sources superimposed on the *Spitzer* 8 μm image. Class 0, IM, and I objects (see Se
plotted as plus circles, squares, and circles, respectively.

Liu+2017

膨張によるバブル非対称構造の解釈

A&A 566, A75 (2014)

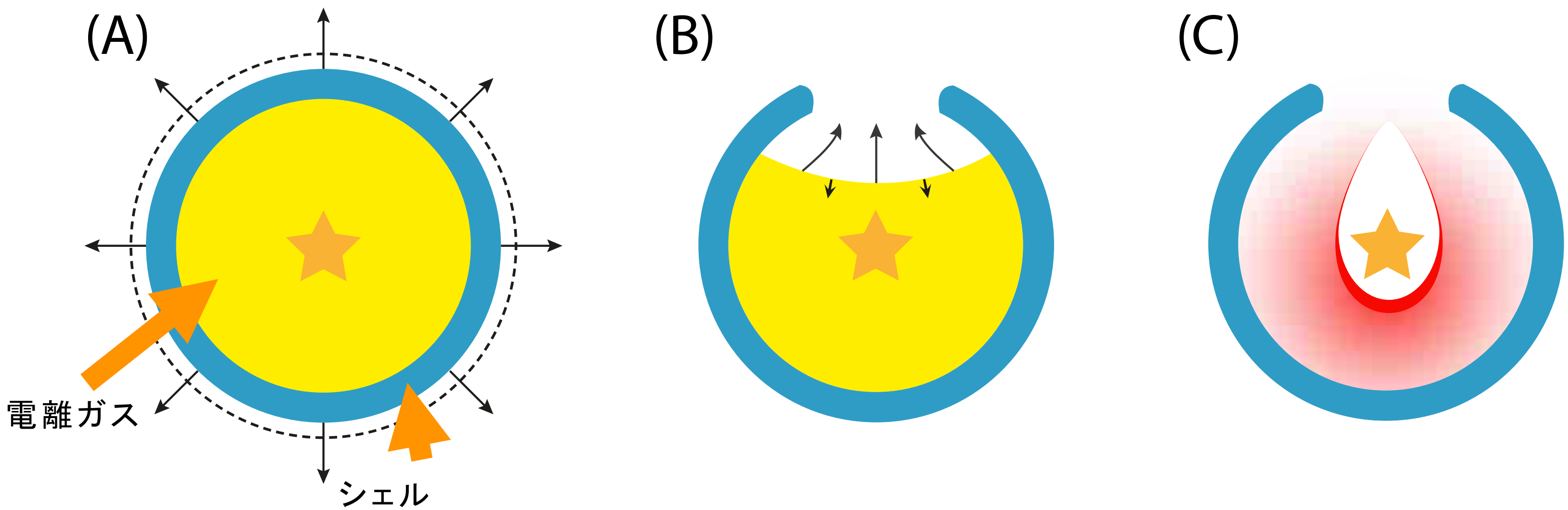

Fig. 2. A) Overpressure of the hot, ionized interior (yellow) will cause the bubble to expand inside the natal cloud, sweeping up neutral gas in a dense shell (blue) (Spitzer 1978). If the expansion is supersonic, a shock front forms on the neutral side of the shell (dashed line). **B)** If the ionized gas contains a density gradient and/or the bubble is punctured, a flow of ionized gas will stream towards lower density and ultimately into the surrounding ISM, relieving the bubble from its pressure (Tenorio-Tagle 1979). **C)** Dust is dragged along in an ionized flow, where "upstream" dust approaching the ionizing source will be heated and halted by radiation pressure, resulting in a *dust wave* or *bow wave* (Ochsendorf et al. 2014; and see Sects. 3.2 and 4), which can be traced at mid-infrared wavelengths (red).

Ochsendorf+ 2014

バブル中心からOffset した励起星からの膨張シミュレーション

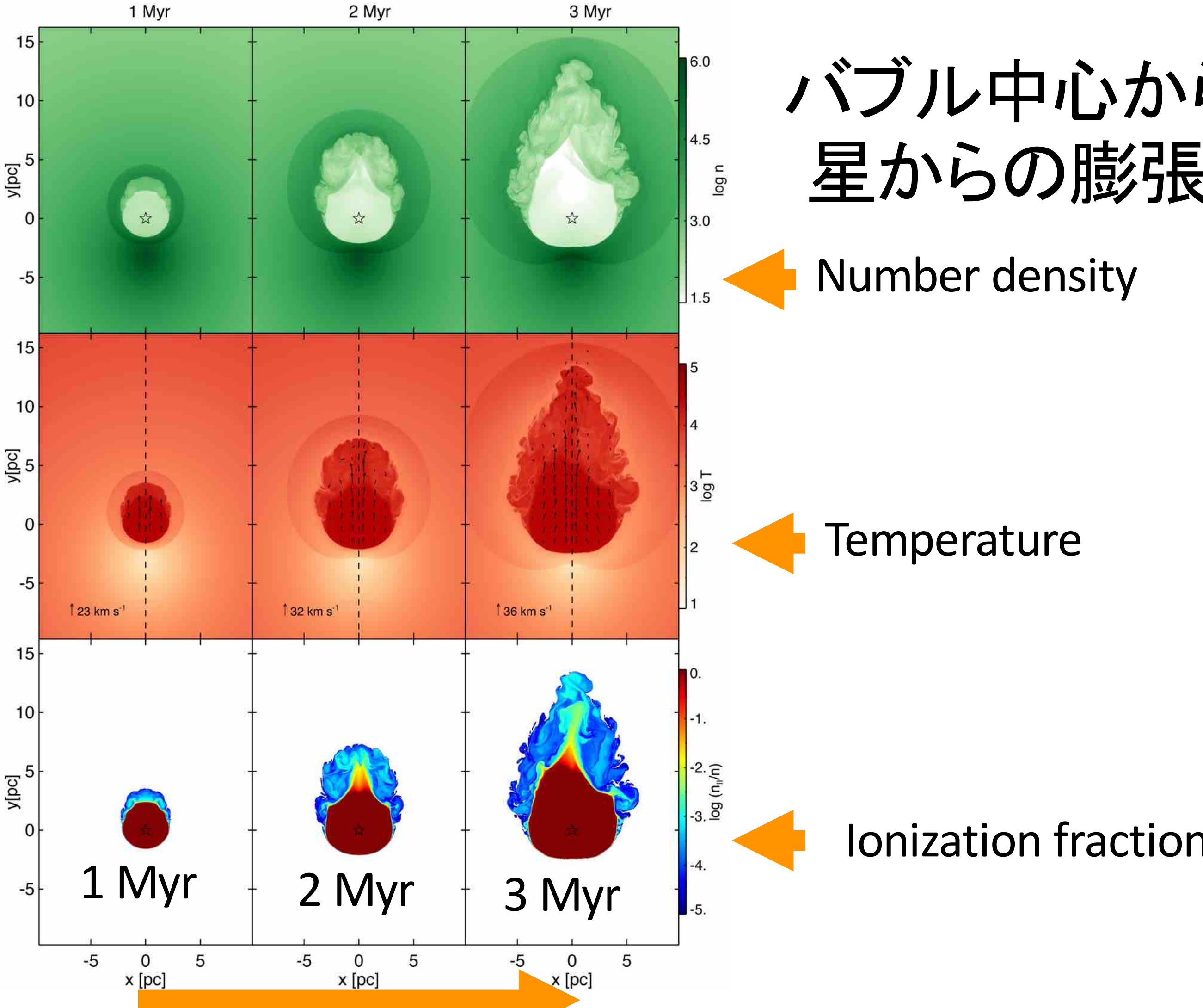

Fig. 3. Two-dimensional hydrodynamical simulation of an expanding H II region offset from the center of a Bonnor-Ebert sphere. *From top to bottom rows*: the logarithm of number density n, temperature T, and ionization fraction $n_{\rm II}/n$ of a slice through the yz-plane at the location of the star are shown. We trace the velocity of the gas in the three-dimensional simulation along the dashed line (see Fig. 4A). Each column corresponds to a snapshot of the simulation at 1–3 Myr. The vectors represent the velocity field in the *middle row*; the legend indicates the maximum velocity.

Ochsendorf+ 2014